NASA/TM—1999-209633

Flutter and Forced Response Analyses of Cascades Using a Two-Dimensional Linearized Euler Solver

T.S.R. Reddy and R. Srivastava
The University of Toledo, Toledo, Ohio

O. Mehmed
Glenn Research Center, Cleveland, Ohio

November 1999

The NASA STI Program Office . . . in Profile

Since its founding, NASA has been dedicated to the advancement of aeronautics and space science. The NASA Scientific and Technical Information (STI) Program Office plays a key part in helping NASA maintain this important role.

The NASA STI Program Office is operated by Langley Research Center, the Lead Center for NASA's scientific and technical information. The NASA STI Program Office provides access to the NASA STI Database, the largest collection of aeronautical and space science STI in the world. The Program Office is also NASA's institutional mechanism for disseminating the results of its research and development activities. These results are published by NASA in the NASA STI Report Series, which includes the following report types:

- TECHNICAL PUBLICATION. Reports of completed research or a major significant phase of research that present the results of NASA programs and include extensive data or theoretical analysis. Includes compilations of significant scientific and technical data and information deemed to be of continuing reference value. NASA's counterpart of peer-reviewed formal professional papers but has less stringent limitations on manuscript length and extent of graphic presentations.

- TECHNICAL MEMORANDUM. Scientific and technical findings that are preliminary or of specialized interest, e.g., quick release reports, working papers, and bibliographies that contain minimal annotation. Does not contain extensive analysis.

- CONTRACTOR REPORT. Scientific and technical findings by NASA-sponsored contractors and grantees.

- CONFERENCE PUBLICATION. Collected papers from scientific and technical conferences, symposia, seminars, or other meetings sponsored or cosponsored by NASA.

- SPECIAL PUBLICATION. Scientific, technical, or historical information from NASA programs, projects, and missions, often concerned with subjects having substantial public interest.

- TECHNICAL TRANSLATION. English-language translations of foreign scientific and technical material pertinent to NASA's mission.

Specialized services that complement the STI Program Office's diverse offerings include creating custom thesauri, building customized data bases, organizing and publishing research results . . . even providing videos.

For more information about the NASA STI Program Office, see the following:

- Access the NASA STI Program Home Page at ***http://www.sti.nasa.gov***

- E-mail your question via the Internet to help@sti.nasa.gov

- Fax your question to the NASA Access Help Desk at (301) 621-0134

- Telephone the NASA Access Help Desk at (301) 621-0390

- Write to:
  NASA Access Help Desk
  NASA Center for AeroSpace Information
  7121 Standard Drive
  Hanover, MD 21076

NASA/TM—1999-209633

Flutter and Forced Response Analyses of Cascades Using a Two-Dimensional Linearized Euler Solver

T.S.R. Reddy and R. Srivastava
The University of Toledo, Toledo, Ohio

O. Mehmed
Glenn Research Center, Cleveland, Ohio

National Aeronautics and
Space Administration

Glenn Research Center

November 1999

Acknowledgments

The authors acknowledge the many helpful suggestions from Dr. M. Montogomery and Dr. V. Capece during the course of using LINFLX2D. This work is supported by a grant from the NASA Glenn Research Center Structural Mechanics and Dynamics Branch under funding from the Advanced Subsonic Technology Project and the Turbomachinery and Combustion Technology Project. John Rohde, George Stefko, and Kestutis Civinskas are the program managers.

Available from

NASA Center for Aerospace Information
7121 Standard Drive
Hanover, MD 21076
Price Code: A03

National Technical Information Service
5285 Port Royal Road
Springfield, VA 22100
Price Code: A03

FLUTTER AND FORCED RESPONSE ANALYSES OF CASCADES USING A TWO DIMENSIONAL LINEARIZED EULER SOLVER

T. S. R. Reddy* and **R. Srivastava***
The University of Toledo
Toledo, Ohio 43606

O. Mehmed†
National Aeronautics and Space Administration
Glenn Research Center
Cleveland, Ohio 44135

ABSTRACT

Flutter and forced response analyses for a cascade of blades in subsonic and transonic flow is presented. The structural model for each blade is a typical section with bending and torsion degrees of freedom. The unsteady aerodynamic forces due to bending and torsion motions, and due to a vortical gust disturbance are obtained by solving unsteady linearized Euler equations. The unsteady linearized equations are obtained by linearizing the unsteady non-linear equations about the steady flow. The predicted unsteady aerodynamic forces include the effect of steady aerodynamic loading due to airfoil shape, thickness and angle of attack. The aeroelastic equations are solved in the frequency domain by coupling the unsteady aerodynamic forces to the aeroelastic solver MISER. The present unsteady aerodynamic solver showed good correlation with published results for both flutter and forced response predictions. Further improvements are required to use the unsteady aerodynamic solver in a design cycle.

INTRODUCTION

The aeroelastic research program at NASA Glenn Research Center is focused on flutter (unstalled, stalled, and whirl), and forced response analyses of propulsion components. An overview of this research was presented in Ref. 1. The review showed that a range of aerodynamic and structural models have been used to obtain the aeroelastic equations. Both, frequency and time domain methods have been used to obtain unsteady aerodynamic forces and to solve the aeroelastic equations. It was noted that time domain methods require large computational time compared to frequency domain methods, and should only be used when non-linearities are expected, or for the final design.

Two approaches have been used in obtaining the unsteady aerodynamic forces using frequency domain methods. In the first approach, Refs. 2-6, the unsteady aerodynamic equations are linearized about a uniform steady flow, thereby neglecting the effects of airfoil shape, thickness, and angle of attack. The unsteady aerodynamic models developed in Refs. 2-6 have been used in Refs. 7-8 to study the flutter and forced response analysis of a compressor cascade using a typical section structural model. However, methods developed by this approach are restricted to shock-free flows through lightly-loaded blade rows. In the second approach, Ref. 9, the unsteady flow

---

* Resident Research Associate, NASA Glenn Research Center, Cleveland, Ohio
† Research Engineer

is regarded as a small amplitude perturbation about a non-uniform steady flow. The unsteady non-linear aerodynamic equations are linearized about the non-uniform steady flow, resulting in variable coefficient linear unsteady aerodynamic equations, which include the effects of steady aerodynamic loading due to airfoil shape, thickness and angle of attack.

Following the second approach, Refs. 10-11 developed a nonlinear steady and linear unsteady aerodynamic model based on the potential equation. This unsteady aerodynamic model was used to study the effect of steady aerodynamic loading on flutter stability using a typical section structural model in Ref. 12. However, the formulation based on the potential equation requires corrections for entropy and flow rotation. The Euler equations can be used to correctly model rotational and entropy effects associated with strong shocks. Unsteady linearized Euler aerodynamic models that include the effect of steady aerodynamic loading were developed in Refs. 13-15.

Recently, a two dimensional linearized Euler code named LINFLX2D was developed (Ref. 16) under a NASA contract. This code is based on the non-linear Euler solver, NPHASE (Ref. 17). The objectives of the present study are (1) to couple the LINFLX2D code with the aeroelastic code MISER (Refs. 7,8 , (2) validate the aeroelastic predictions, and (3) evaluate the LINFLX2D code for use in the aeroelastic design cycle. The MISER code at present calculates the flutter and forced response characteristics using the unsteady aerodynamic models based on classical linear theories (theories based on flat plate geometry formulation). The MISER code is selected because the typical section structural model with pitching and plunging degrees of freedom is the basis for aeroelastic formulation. This is in line with the unsteady aerodynamic model of LINFLX2D. Over the years, many versions of MISER have been in circulation. To show that the version of the MISER code used in the present calculations gives correct results, selected cases from Ref. 7 are recalculated and the results presented in Appendix A.

In the current report flutter and forced response analyses of a cascade of blades is presented using the frequency domain approach for a two-dimensional cascade model. Two degrees of freedom, plunging and pitching, are considered in the analysis. Vortical gust disturbance is considered for forced response calculations. Brief descriptions of the formulation and method of analysis are given in the next section, followed by results and discussion.

FORMULATION

The aerodynamic model and the aeroelastic formulation are described in this section.

Aerodynamic model

Non-linear Steady Euler Solver, NPHASE

The steady aerodynamic model is based on the unsteady, two-dimensional Euler equations. The equations in conservative differential form are solved in a time-dependent body-fitted curvilinear reference frame. This transformation process and the ensuing numerical method are presented in detail in Ref. 17. The equations are discretized and solved using a finite volume method using a TVD scheme. The steady solutions presented herein are obtained using the implicit scheme developed in Ref. 17, which is third order accurate in space and second order accurate in time.

Linear Unsteady Euler Solver, LINFLX2D

To obtain the linearized unsteady Euler equations, Ref. 16, the dependent variables in the unsteady non-linear Euler equations are expanded in an asymptotic series of the form

$$U = U(x) + u(x(x,t),t) + \quad \text{higher order terms} \tag{1}$$

where, the term U(x) is of order one and the second term is of the order ε. Substituting the expansion of Eq. 1 in the nonlinear unsteady Euler equations, and equating terms of like power in ε, and neglecting terms of second and higher order in ε, nonlinear steady equations and linear variable coefficient unsteady equations are obtained. The unsteady linear equations are further simplified by assuming the unsteady excitations and responses are harmonic in time as

$$u(x(x,t),t) = \mathrm{Re}[u(x)\exp(i\omega t) \tag{2}$$

For harmonic blade motions with constant phase angle between adjacent blades (interblade phase angle), the values of interblade phase angle (σ) that can occur are given as (Ref. 18).

$$\sigma_r = 2\pi r / N \qquad r = 0,1,2, ..., N\text{-}1 \tag{3}$$

where N is the number of blades in the cascade. In a time domain approach, the number of blade passages required for the solution depends on the interblade phase angle, and small phase angles may require a large number of blade passages to calculate the unsteady aerodynamic forces. However, with the linear approach, the periodic conditions are applied on a single extended blade passage region i.e. a region of angular pitch,

$$\theta = 2\pi / N \tag{4}$$

In solving the linear unsteady equations, the independent variables are regarded as pseudo time dependent. This allows solutions to be determined using conventional time -marching algorithms to converge the steady and the complex amplitudes of the unsteady conservation variables to their steady state values. For more details, see reference 16.

Aeroelastic model

For completeness, the aeroelastic formulation in the frequency domain for a typical section structural model (Refs. 7,8) is presented in this section. The analysis is presented for a generally mistuned cascade in which each blade may have different structural properties. The analysis for the special case of a tuned cascade in which all blades are identical is presented in the subsequent section. The approach followed assumes that the structure is vibrating in an aeroelastic mode (interblade phase angle mode) with a motion that is a harmonic function of time. The frequency of oscillation is permitted to take on complex values thus allowing decaying-, growing- or constant-amplitude oscillations. The aerodynamic forces corresponding to constant-amplitude harmonic oscillations are inserted into the equations of motion to formulate a complex eigenvalue problem. The eigenvalues are generally complex quantities, and therefore a complex frequency is obtained. The real part of the complex frequency represents the damping ratio and thus its sign determines whether the motion is decaying or growing; the imaginary part represents the damped frequency of oscillation.

Aeroelastic analysis for mistuned cascade

The equations of motion for the typical section (see Fig. 1) with structural damping can be written in matrix form for the s^{th} blade as:

$$[M_s]\{\ddot{q}_s\}+[C_s]\{\dot{q}_s\}=[K_s]\{q_s\}=\left\{f_{as}^{q}\right\}=\{f_{as}\} \tag{5}$$

where $\{f_a{}^q\}$ denotes motion-dependent aerodynamic loads and $\{fa\}$ denotes motion-independent aerodynamic loads.

For the two degrees of freedom considered here, equation 5 can be rewritten as

$$\begin{bmatrix} 1 & x_{\alpha s} \\ x_{\alpha s} & r_{\alpha s}^2 \end{bmatrix}\begin{Bmatrix} \ddot{h}_s/b \\ \ddot{\alpha}_s \end{Bmatrix}+\begin{bmatrix} 2\omega_{hs}\zeta_{hs} & 0 \\ 0 & 2r_{\alpha s}^2\omega_{\alpha s}\zeta_{\alpha s} \end{bmatrix}\begin{Bmatrix} \dot{h}_s/b \\ \dot{\alpha}_s \end{Bmatrix}+\begin{bmatrix} \omega_{hs}^2 & 0 \\ 0 & r_{\alpha s}^2\omega_{\alpha s}^2 \end{bmatrix}\begin{Bmatrix} h_s/b \\ \alpha_s \end{Bmatrix}=\begin{Bmatrix} f_{hs}/m_s b \\ f_{\alpha s}/m_s b^2 \end{Bmatrix} \tag{6}$$

where h is the plunging (bending) displacement normal to the chord, α is the pitching (torsion) displacement, x_α the distance between the elastic axis and center of mass in semi-chord units; r_α is the radius of gyration about the elastic axis in semi-chord units; ζ_h and ζ_α are the damping ratios; b is the airfoil semi-chord; ω_h is the uncoupled natural frequency for bending; ω_α is the uncoupled natural frequency for torsion; f_h and f_α are the aerodynamic loads.

It is assumed that the motion of the blades is harmonic in time with a frequency ω and is given by

$$\begin{Bmatrix} h_s/b \\ \alpha_s \end{Bmatrix}=\begin{Bmatrix} h_{0s}/b \\ \alpha_{0s} \end{Bmatrix}e^{i\omega t}=\sum_{r=0}^{N-1}\begin{Bmatrix} h_{ar}/b \\ \alpha_{ar} \end{Bmatrix}e^{i\omega t}e^{i\sigma_r s} \tag{7}$$

Note that the motion has been represented as the sum of contributions from each interblade phase angle mode in which each blade has an amplitude h_{ar}/b, α_{ar} and the phase angle between adjacent blades is given by Eq. 3.

The corresponding aerodynamic forces can be written in terms of the complex-valued unsteady aerodynamic coefficients l_{hh} , $l_{\alpha h}$, $l_{h\alpha}$, $l_{\alpha\alpha}$, l_{wh}, and $l_{w\alpha}$ (see Ref. 7 for the definition of these coefficients) as

$$\begin{Bmatrix} f_{hs}/m_s b \\ f_{\alpha s}/m_s b^2 \end{Bmatrix}=\frac{\omega^2}{\mu_s}\sum_{r=0}^{N-1}\begin{Bmatrix} [l_{hhr}h_{ar}/b+l_{h\alpha r}\alpha_{ar}] \\ [l_{\alpha hr}h_{ar}/b+l_{\alpha\alpha r}\alpha_{ar}] \end{Bmatrix}e^{i\omega t}e^{i\sigma_r s}+\frac{\omega^2}{\mu^2}\sum_{r=0}^{N-1}\begin{Bmatrix} [l_{whr}] \\ [l_{w\alpha r}] \end{Bmatrix}e^{i\omega t}e^{i\sigma_r s} \tag{8}$$

where $\mu_s = m_s/\pi\rho_\infty b^2$ is the mass ratio of the blade, and ρ_∞ is the density of air.

Using Eq. 7 and Eq. 8, Eq. 6 can be written as

$$-[M_s]\begin{Bmatrix} h_{os}/b \\ \alpha_{os} \end{Bmatrix} e^{i\omega t} + \lambda\,[K_s]\begin{Bmatrix} h_{os}/b \\ \alpha_{os} \end{Bmatrix} e^{i\omega t}$$

$$= \sum_{r=0}^{N-1} [A_r]\begin{Bmatrix} h_{or}/b \\ \alpha_{or} \end{Bmatrix} e^{i\sigma s} e^{i\omega t} + \sum_{r=0}^{N-1} \{AD_r\} e^{i\sigma s} e^{i\omega t} \qquad (9)$$

where

$$[M_s] = \mu_s \begin{bmatrix} 1 & x_\alpha \\ x_\alpha & r_\alpha^2 \end{bmatrix} \qquad [K_s] = \begin{bmatrix} (\omega_{hs}/\omega_b)^2 (1+2i\zeta_{hs}) & 0 \\ 0 & r_{\alpha s}^2 (\omega_{\alpha s}/\omega_b)^2 (1+2i\zeta_{\alpha s}) \end{bmatrix}$$

$$[A_r] = \begin{bmatrix} l_{hhr} & l_{h\alpha r} \\ l_{\alpha hr} & l_{\alpha\alpha r} \end{bmatrix} \qquad \{AD_r\} = \begin{Bmatrix} l_{whr} \\ l_{w\alpha r} \end{Bmatrix} \qquad \lambda = (\omega_b/\omega)^2$$

where ω_0 is the reference frequency and the damping terms are approximated as,

$$2i\omega\omega_{hs}\zeta_{hs} \approx 2i\omega_{hs}^2\,\zeta_{hs}$$
$$2ir_{\alpha s}^2\omega\omega_{\alpha s}\zeta_{\alpha s} \approx 2ir_{\alpha s}^2\,\omega_{\alpha s}^2\zeta_{\alpha s} \qquad (10)$$

To proceed further, the equations for all the *N* blades on the disk must be considered. For the assumed harmonic blade motion, the displacements {X} of all blades can be written as a sum of contributions from all interblade phase angles as

$$\{X\}e^{i\omega t} = [E]\{Y\}e^{i\omega t} \qquad (11)$$

where {Y} consists of the displacement amplitudes corresponding to the rth interblade phase angle and [E] is the transfer matrix, the elements of which are given by

$$E(s,r) = e^{2\pi sri/N}$$

where s is the blade counter and r is the interblade phase angle counter.

Using this relation, we obtain:

$$-[E]^{-1}[M][E]\{Y\} + \lambda\;[E]^{-1}[K][E]\{Y\} = [A]\{Y\} + \{AD\} \qquad (12)$$

where

[M] is the mass matrix for all blades with diagonal elements consisting of mass matrix of each blade. Similarly [K] is the stiffness matrix and [A] is the aerodynamic matrix for all blades, {AD} is the aerodynamic forces due to wake on all the blades.

Finally, after rearranging, the equations can be written as:

$$\left[[P]-\lambda\,[Q]\right]\{Y\} = -\{AD\} \tag{13}$$

where

$$[P] = \left[[E]^{-1}[M][E]+[A]\right]$$

$$[Q] = [E]^{-1}[K][E]$$

For a stability calculation (flutter), the motion-independent forces {AD} are set to zero and the eigenvalue problem is obtained in the standard form:

$$[[P]-\lambda[Q]]\{Y\}=\{0\} \tag{14}$$

The solution of the above eigenvalue problem Eq. 14 results in $2N$ complex eigenvalues of the form

$$i\frac{\omega}{\omega_0} = \frac{i}{\sqrt{\lambda}} = \bar{\mu} + i\,\bar{\nu} \tag{15}$$

The real part of the eigenvalue ($\bar{\mu}$) represents the damping ratio, and the imaginary part ($\bar{\nu}$) represents the damped frequency; flutter occurs if $\bar{\mu} \geq 0$ for any of the eigenvalues.

The aeroelastic response of the blades induced by wakes is calculated from equation (13) as

$$\{Y\} = -\left[[P]-\lambda\,[Q]\right]^{-1}\{AD\} \tag{16}$$

The amplitude of each blade is obtained by substituting equation (16) into equation (11).

Aeroelastic analysis for a tuned cascade

For a tuned cascade (or rotor), in which all the blades are identical, the foregoing analysis can be simplified considerably. In this case, the aeroelastic modes consist of individual blades vibrating with equal amplitudes with a fixed interblade phase angle between adjacent blades. Hence, for this problem, the motion of the typical blade is written as

$$\begin{Bmatrix} h_s/b \\ \alpha_s \end{Bmatrix} = \begin{Bmatrix} h_{0s}/b \\ \alpha_{0s} \end{Bmatrix} e^{i\omega t} = \begin{Bmatrix} h_{ar}/b \\ \alpha_{ar} \end{Bmatrix} e^{i\omega t} e^{i\sigma_r s} \tag{18}$$

Thus the equation for the blade becomes

$$-[M_s]\begin{Bmatrix} h_{ar}/b \\ \alpha_{ar} \end{Bmatrix} e^{i(\omega+\sigma_r s)} + \lambda[K_s]\begin{Bmatrix} h_{ar}/b \\ \alpha_{ar} \end{Bmatrix} e^{i(\omega+\sigma_r s)} = [A_r]\begin{Bmatrix} h_{ar}/b \\ \alpha_{ar} \end{Bmatrix} e^{i(\omega+\sigma_r s)} + \{AD_r\} e^{i(\omega+\sigma_r s)} \tag{19}$$

Since the blades are identical, the same equation is obtained for each blade. Thus, no additional information can be obtained by assembling the equations for all the blades on the disk as was done for the general mistuned system. Instead, equation (19) is solved for N different values of the interblade phase angle given by equation (3). As before, the equations for the stability (flutter) calculation are obtained by setting the motion-independent forces to zero.

For the stability calculation, the equation can be simplified as

$$\left[[P_r] - \lambda [I]\right]\{Y\} = \{0\} \tag{20}$$

where

$$[P_r] = \begin{bmatrix} \dfrac{\mu + l_{hhr}}{\mu(\omega_h/\omega_\alpha)^2(1+2i\zeta_h)} & \dfrac{\mu x_\alpha + l_{h\alpha r}}{\mu(\omega_h/\omega_\alpha)^2(1+2i\zeta_h)} \\ \dfrac{\mu x_\alpha + l_{\alpha h r}}{\mu r_\alpha^2(1+2i\zeta_\alpha)} & \dfrac{\mu r_\alpha^2 + l_{\alpha\alpha r}}{\mu r_\alpha^2(1+2i\zeta_\alpha)} \end{bmatrix}$$

where the subscript *'s'* identifying the blade has been dropped and the reference frequency ω_o has been chosen to be equal to the torsional frequency ω_α.

The solution of the above eigenvalue problem results in two complex eigenvalues of the form $\bar{\mu} + i\,\bar{\nu}$, and flutter occurs if $\bar{\mu} \geq 0$. For the tuned cascade, the stability of each phase angle mode is examined separately. Hence, the interblade phase angle is fixed at one of the values given by equation (3), and the 2X2 eigenvalue problem is solved. The value of interblade phase angle is then changed, and the procedure is repeated for each of the N permissible values. The critical phase angle is identified as the one which results in the lowest flutter speed.

Stability calculation

The aerodynamic coefficients are calculated before the eigenvalue problem can be set up and solved. Since the unsteady aerodynamic coefficients depend on the frequency of oscillation, it is necessary to assume a frequency ω (reduced frequency of blade vibration based on chord, k_c = ω c / U, where U is the free stream velocity) in advance to be able to calculate the aerodynamic coefficients. In actual calculations, the aerodynamic coefficients are functions of inlet Mach number M_∞, and interblade phase angle σ_r, in addition to cascade geometric parameters. In the current study, for a given inlet Mach number, the reduced frequency is varied until the real part of one of the eigenvalues $\bar{\mu}$ becomes zero while the real parts of the remaining eigenvalues are negative. The assumed flutter-reduced frequency k_{cf} and the calculated flutter frequency $\bar{\nu}_f$ are both based on ωf. Thus, these two can be combined to eliminate ωf and the flutter speed is obtained, namely, $V_f = \bar{\nu}_f\, c\, \omega_o / k_{cf}$. Since the inlet Mach number is known, this flutter speed gives the inlet condition (speed of sound, a_∞) at which the cascade will be neutrally stable for the given Mach number. This procedure can be repeated to obtain a plot of flutter speed versus Mach number. Knowing the operating conditions, it is possible to determine whether flutter will

occur within the operating region and if so, the Mach number and frequency at flutter. It should be noted that the analysis of a mistuned cascade requires the solution of the equations for all phase angles at one time for a given reduced frequency.

RESULTS AND DISCUSSION

The analysis methods presented earlier are now applied to investigate the behavior of cascades oscillating in pitch and plunge, and cascades subjected to unsteady vortical gust disturbance. First, unsteady pressure distributions and loading for selected cascade configurations are presented and compared with published results to help validate the present linearized unsteady Euler solver, LINFLX2D. Then, flutter and forced response predictions with and without mistuning are presented. For the calculation of unsteady aerodynamic forces, first NPHASE, the non-linear Euler solver is used to generate the steady solution. This steady solution is then used as an input to LINFLX2D, to calculate the unsteady aerodynamic forces due to small unsteady perturbations in pitch, plunge and vortical gust disturbance. The calculated unsteady aerodynamic coefficients are used in MISER to predict the flutter stability and forced response. The MISER code used in the present investigation has been verified and sample results are presented in Appendix A.

Code Validation

Unsteady pressure difference, the difference between the lower and upper surfaces of the airfoil, were calculated for a flat plate cascade, and a cascade designated as the tenth standard configuration (C10), Ref. 16. The unsteady pressures difference was normalized by ((air density* square of free stream velocity*abs(amplitude of pitching motion + amplitude of plunging motion* k_C)). Both cascades have a stagger angle (θ) of 45 degrees, and a gap to chord ratio (s/c) of 1.0. The tenth standard configuration airfoils are constructed by superposing the thickness distribution of a modified NACA 5506 airfoil on a circular-arc camber line. See Ref. 16 for more details. Two Mach numbers are considered, M=0.7 and M=0.8 for a reduced frequency of oscillation based on semichord (k_b ; k_b = 0.5* k_C) of 0.5. At M=0.7 the flow is subsonic, and at M=0.8 the flow is transonic with a shock at 25% chord from the leading edge of the airfoil. The steady angle of attack is zero for the flat plate geometry. It is ten degrees for the C10 airfoil at M=0.7, and thirteen degrees at M=0.8. Unless otherwise stated, a 141x41 H-grid is used for the study. There are 80 points on the airfoil, the inlet boundary is 5 chords from the airfoil leading edge, and the exit boundary is 10 chords from the airfoil trailing edge. Some calculations were also done with a 155x41 grid for which the inlet and exit boundaries are located at one chord from the leading and trailing edges, respectively. There are 55 points on the airfoil for this grid.

Unsteady Aerodynamic Pressures

Subsonic Inflow

Figure 2a shows the unsteady pressure difference distribution obtained for the flat plate cascade operating at M = 0.7. The interblade phase angle, σ, is 180 degrees, the reduced frequency of oscillation (k_h) is 0.5, and the Mach number is 0.7. The blades are oscillating in pitch about the midchord. For the inlet Mach number of 0.7, the flow is shock free. Figure 2a shows predictions form linear theory (Ref. 3) and from the present linearized Euler code, LINFLX2D. The predictions from LINFLX2D correlate well with the linear theory results.

Figure 2b shows the unsteady pressure difference distribution obtained for the standard cascade configuration, C10. The flow to the cascade is at 10 degrees angle of attack. Again, the interblade phase angle is 180 degrees, the reduced frequency of oscillation (k_h) is 0.5, and the Mach number of 0.7. The blades are oscillating in pitch about the midchord. For the inlet Mach number of 0.7, the flow is shock free. Figure 2b shows predictions from linear theory (Ref. 3), nonlinear Euler (Ref. 17) and from the present linearized Euler code, LINFLX2D. The predictions from LINFLX2D correlate well with the nonlinear Euler results. As expected, there is a difference with linear theory, since the effects of airfoil geometry and angle of attack are not included in the linear theory.

Transonic Inflow

For the standard configuration, C10, and for an inlet Mach number of 0.8, the flow is transonic with a normal shock occurring in each blade passage. The steady angle of attack is 13 degrees. The steady Mach number distribution for this flow obtained from NPHASE is shown in Fig. 3a. There is a normal shock at about 28% of the chord. Results from the full potential solver, Ref. 19, are also included for comparison. Both results agree well, except that the nonlinear steady Euler solver, NPHASE, predicts the shock location slightly downstream of that predicted by the full potential solver. A shock fitting procedure was used in Ref. 19, whereas the shock is captured in the present solver.

The unsteady pressure distribution from LINFLX2D is shown in Fig. 3b, along with a comparison with linear theory (Ref. 3) and from the unsteady nonlinear Euler solver (Ref. 17). The unsteady results are for pitching about mid-chord with $k_b = 0.5$, $\sigma = 180°$ and amplitude of oscillation, $\alpha_o = 2°$. As expected, linear theory does not show any shock, indicating that unsteady analysis based on linear theory will not be accurate for cascade flutter analysis in transonic flow. Some discrepancy is seen between the unsteady results obtained from LINFLX2D and from the unsteady nonlinear Euler solver. For the transonic flow case the following factors may effect the results more than for subsonic case: (1) grids used, (2) accuracy lost when time series data is processed to obtain frequency data or (3) the steady solution on which LINFLX2D based is not a low loss solution. Even though these issues need separate study, Fig. 3b shows a fair correlation between LIFLX2D results and non-linear unsteady Euler.

Similar results were obtained for plunging motion for both subsonic and transonic inflows.

Unsteady Aerodynamic Force coefficients

It is the unsteady aerodynamic force coefficients, unsteady lift and moment that are obtained by integrating unsteady pressure differences, which are used in the flutter and forced response prediction. Table 1 shows the unsteady aerodynamic force coefficients obtained using the Smith code, Ref. 3, the present LINFLX2D code, and the non-linear Euler solver of Ref. 17. In table 1, the first column shows the geometry of the airfoil studied, the fourth, fifth and sixth columns show the force components for pitching motion, plunging motion and for vortical gust respectively. The symbols in the second column are *cl* for lift coefficient, and *cm* for moment coefficient, with moment taken about the mid chord ($x_{ii} = 0.5$). The rows show the geometry and the Mach number studied. The analysis method is given in column 3 with the notation defined at the bottom of the table. The geometry and unsteady conditions are given on the top of the table.

A comparison of the force coefficients for flat plate geometry in the first row shows that the prediction by LINFLX2D are very close to those given by Smith code. For a flat plate geometry in subsonic flow, the Smith code gives the exact answer. It is to be noted that the flat plate is unloaded and shock free. The values of the force coefficients in the second row show some difference from the Smith code, since in LINFLX2D the effect of airfoil and angle of attack are included. The force coefficients in the third row include the effect of shock and its motion in addition to the effects of airfoil shape and angle of attack. The force coefficients obtained with LINFLX2D code compare well with those obtained from a non-linear unsteady Euler solution, indicating that LINFLX2D code can be used to analyze cascades in transonic flow. It is to be noted that only limited runs for vortical gust response predictions have been made. It is also to be noted that the solution for transonic flow could not be obtained with 155x41 grid considered here for which the inlet and exit boundaries are at one chord length. It was suggested that for the LINFLX2D code to work properly, it is better if the inlet and exit boundaries are at least 5 chords from the leading and trailing edges respectively (Ref. 20).

Flutter Calculations

As mentioned before, given the unsteady aerodynamic force coefficients, the MISER code (Ref. 7) calculates the aeroelastic stability of tuned and mistuned cascades oscillating in pitch and plunge. The aeroelastic stability results from MISER are presented as a root locus plot, with real part of the eigenvalue indicating damping and the imaginary value indicating frequency for all possible interblade phase angles. In the present study the unsteady aerodynamic force coefficients obtained from LINFLX2D are coupled with MISER as follows. First a steady solution is obtained from NPHASE for the required cascade geometry and flow conditions. With the steady solution as input, LINFLX2D is run for given a reduced frequency, interblade phase angle, and mode of interest (pitching or plunging). The unsteady aerodynamic coefficients obtained from LINFLX2D are then stored in a data base, and later used in MISER to calculate the stability characteristics.

The structural properties are the mass ratio, μ, is 258.50; ratio of bending to torsion frequencies, ω_h / ω_α is 0.357; the radius of gyration about the elastic axis in semi-chord units, r_α, is 0.5774; with no structural damping. The elastic axis (see Fig. 1) is at midchord, i.e. ah = 0.0. The distance between the elastic axis and center gravity, x_α is zero, indicating that coupling between bending and torsion is very weak and the flutter mode is dominated by torsional motion.

Therefore, only torsion mode is shown for all the calculations. It should be noted that these structural properties were also used in Refs. 7 and 8.

The following procedure is used for stability prediction. First MISER is run for the selected cascade (rotor) using linear theory (Ref. 3) to identify the flutter point. Then MISER is run using the LINFLX2D data base for this flutter condition. The eigenvalues obtained from linear theory and LINFLX2D are then compared.

Flat Plate Cascade

To validate the coupling of the unsteady aerodynamic coefficients obtained from LINFLX2D with MISER, a nine bladed cascade with a flat plate geometry was selected. The flutter results obtained are compared with those obtained from linear theory. The gap-to-chord ratio is unity and the stagger angle is 45 degrees. For the nine bladed cascade, for a given reduced frequency, the unsteady force coefficients have to be calculated for the possible interblade phase angles of 0, 40, 80, 120, 160, 200, 240, 280, and 320 degrees.

Using linear theory, for M = 0.7 with elastic axis at midchord, for the nine bladed cascade mentioned above, an instability was found at k_h = 0.18 and at a phase angle of 80 degrees. Therefore, LINFLX2D was run for this value of reduced frequency, and for all allowable phase angles, and for both plunging and pitching oscillations, and a database was prepared. Then MISER was run to predict the stability boundary with the unsteady aerodynamic force coefficient data base obtained from LINFLX2D.

The root locus plot showing the real and imaginary parts of the eigenvalues for the flat plate geometry obtained for torsion motion is given in Fig. 4. The unsteady force coefficients for eight phase angles were obtained with LINFLX2D. For the σ = 40 degrees, for which acoustic resonance was expected, the LINFLX2D code did not give a solution for the grid, oscillation of amplitude, and time step considered. This case will be studied further in future. It was noted that for a flat plate geometry, the computational times were higher than those for airfoil geometry (presented below). Figure 4 shows the comparison between predictions from linear theory and from LINFLX2D. It can be seen from Fig. 4 that LINFLX2D compares very well with linear theory results for the flat plate geometry. The plot shows that the cascade is unstable at the 80° phase angle mode.

Mistuned Cascade

Results are presented now for cascades with mistuning. The type of mistuning considered is the one in which the odd and even numbered blades have different torsional frequencies, also known as alternate blade mistuning. This has been studied in Refs. 7 and 8 with 1% and 1.5% alternate mistuning. For 1% mistuning, the frequency ratio $\omega_\alpha / \omega_\alpha$ is 1.005 for all the even blades, and is 0.995 for all the odd blades. The study in Ref. 7 and 8 considered a 56 bladed cascade, and showed that alternate mistuning has a considerable effect on stability. A 12 bladed cascade is considered for the present study, to limit the computational time. MISER was run first for a tuned cascade with linear theory, for M=0.7. It was found that the cascade is unstable for k_h = 0.1 and σ = 60°. This value of k_h = 0.1 is used for all the calculation presented below. It should be noted here that for this cascade acoustic resonance was expected for σ = 0° and 30°. However, for the C10 airfoil geometry unsteady solutions were obtained with LINFLX2D for these

interblade phase angles also, unlike for the flat plate geometry for which solutions could not be obtained with LINFLX2D at acoustic resonance (as mentioned in the previous section).

First, the amount of mistuning required to change the root locus plot is investigated, i.e., whether the effects of 1% and 1.5% alternate as reported in Ref. 7 also occurs for this cascade. It should be noted here that the results from the present MISER code were checked with those given in Ref.7 for the 56 bladed cascade before starting the current calculations, and are given in Appendix A for both flutter and forced response calculations. Figure 5 shows the root locus plot with 1%,1.5%,5%,10% and 20% alternate mistuning for the flat plate geometry for M = 0.7 and k_b = 0.18. It can be seen that an alternate mistuning of 1-10% did not show any effect on the eigenvalues. Only 20% alternate mistuning showed some effect on the eigenvalues. This is in contrast to the level of mistuning used in Ref. 7. However, Ref. 7 has considered a 56 bladed cascade in incompressible flow for which the cascading effect is much stronger.

However, the large amount of mistuning required here to have a significant effect on the eigenvalues (shown in Fig. 5) is not surprising. Similar values of mistuning have been used in Ref. 8. That study used an amount of 1 to 20% mistuning. An examination of Fig. 11 of Ref. 8 showed that the effect of alternate mistuning decreased with increasing Mach number. In the context of Ref. 8 and the present results, it is concluded that for the Mach numbers considered here a mistuning of 20% or more has to be used to show a significant effect of on the eigenvalues. Therefore, the rest of the calculations are done with 20% alternate mistuning.

Figure 6 shows the root locus plot obtained for the C10 airfoil for both tuned and 20% alternate mistuning, for M = 0.7 and k_b = 0.1. Comparison with flat plate geometry is also shown. The following are noted from Fig. 6: (1) For the tuned cascade both flat plate geometry cascade and C10 airfoil cascade are unstable for $\sigma = 60^\circ$. However, the C10 cascade is less unstable than the flat plate cascade. This indicates that for the tuned cascade the airfoil steady loading effects are stabilizing, compared to that for a flat plate airfoil; (2) the addition of 20% alternate mistuning moved the cascade with C10 geometry from an unstable to a stable condition, but the flat plate cascade remained unstable; (3) the root locus plot for the C10 airfoil with mistuning has two frequencies identified with a $\sigma = 240^\circ$ mode, whereas, the $\sigma = 60^\circ$ mode is completely missing. The reason for this behavior is under investigation.

The root locus plot for M = 0.8 and k_b = 0.1 is shown in Fig. 7. The following are noted form Fig. 7: (1)the tuned flat plate geometry cascade was unstable for $\sigma = 90^\circ$ and the C10 airfoil cascade was stable. This indicates that the airfoil steady loading effects are stabilizing for the tuned cascade, compared to that for a flat plate airfoil; (2) the addition of alternate mistuning made the C10 geometry more stable, but the flat plate cascade remained unstable; (3) For the C10 airfoil it was noted that for tuned case both $\sigma = 90^\circ$ and $\sigma = 120^\circ$ modes have the same amount of damping, but with mistuning, $\sigma = 90^\circ$ mode became more stable than the $\sigma = 120^\circ$ mode.

Forced Response Calculations

In the formulation for response prediction in MISER, it is possible to consider an excitation function consisting of all harmonics of rotational speed of the rotor which range up to r = N-1. In engine aeroelastic terminology, the harmonic number r is known as the " engine order " of the

excitation. The number of harmonics and interblade phase angles are related by Eq. 3 as $\sigma_r = 2\pi r / N \quad r = 0, 1, 2, \cdots, N-1$. The coefficients l_{whr} and $l_{w\alpha r}$ in Eq. 8 represent the forcing functions in the bending and torsion equations, respectively. To understand the nature of the response, excitation in only one harmonic at a time is considered. This results in no loss of generality since the principle of superposition holds. If the r = R harmonic is considered, then the column matrices $\{AD_0\}$, $\{AD_1\}$,...,$\{AD_{N-1}\}$ are zero except $\{AD_r\}$. Generally, a limited number of engine order of excitations are of interest in forced response calculations. Thus, all harmonics or all interblade phase angle modes *need not be* considered in forced response analysis, as in flutter analysis. In the following only torsional response amplitudes are shown since bending amplitudes are very small in the range of excitation frequency considered.

Figure 8 shows the tuned aeroelastic response for R = 6 i.e. σ = 180 degrees for flat plate geometry. Again a twelve blade (N = 12) cascade with the same structural properties used for flutter calculations is considered. However, a structural damping ratio of 0.002 is included in the analysis. The unsteady aerodynamic coefficients are obtained at $k_b = 0.5$ for which the cascade is aeroelastically stable in all the modes. Calculations are done with a 155x41 grid for which the inlet and exit boundaries are located at one chord from the leading and trailing edges respectively. There are 55 points on the airfoil for this grid. The forcing frequency range investigated is limited to a small range around the uncoupled torsional frequency. For the tuned cascade, the response will be entirely in the r = R mode, and all the blades will have equal amplitudes. The amplitude of response is a function of ω / ω_α. Figure 8 shows the torsional response obtained using linear (Smith) theory and present LINFLX2D code for vortical gust disturbance. The moments are taken about leading edge (ah = -1.0). Two responses are shown in Fig. 8 one obtained by including the motion dependent aerodynamic matrix [A] in Eq. 12 and the other without the contribution from [A]. The terms of [A] provide aerodynamic damping in response calculations. It can be seen that calculations from Smith theory and from LINFLX2D are identical indicating that the coupling of LINFLX2D coefficients to MISER code is accurate.

The inclusion of [A] in response calculations requires the calculation of motion dependent unsteady aerodynamic coefficients for all interblade phase angles. However, as mentioned earlier, in forced response calculations, only a limited number of interblade phase angles (engine orders) are of interest and the calculations of motion dependent unsteady aerodynamic coefficients is unnecessary. This essentially ignores the effect of aerodynamic damping on response. As forced response is usually calculated for an aeroelastically stable system (positive aerodynamic damping), this gives a conservative measure on the response calculations. Therefore for further calculations the elements of matrix [A] are not included in the calculation.

Figure 9 shows the torsional response obtained for the standard configuration in subsonic flow with and without 20% alternate mistuning. Comparing the response of C10 with that of flat plate, it can be seen that the response has increased considerably. This may be due to high steady loading on the airfoil. Also shown in Fig. 9 is the response with 20% alternate mistuning. The response has split into two resonance peaks, one for odd blades and the other for even blades, resonating at the 0.9 and 1.1 frequency ratios, as expected with no difference in amplitude. It should be noted that the study of Ref. 7 showed that when the aerodynamic damping terms are included in the response calculations, the amplitudes could be lower or higher depending on the engine order.

The calculations given above for flat plate geometry show that the LINFLX2D data base is accurately coupled with MISER for forced response calculations, as was shown for flutter calculations in the previous section.

CONCLUDING REMARKS

A two-dimensional unsteady linearized aerodynamic Euler solver, LINFLX2D was used to calculate unsteady aerodynamic forces on oscillating cascades. The unsteady aerodynamic forces were used in the aeroelastic code MISER to calculate flutter and forced response characteristics of cascades. Results were presented for cascades in subsonic and transonic flow. Calculations with the linearized Euler solver showed good correlation with the published data. The study also showed that the unsteady aerodynamic force data base (for flutter and forced response) from LINFLX2D is successfully coupled with MISER to calculate flutter and forced response of tuned and mistuned cascades. The following were observed during the study.

(1) The airfoil steady loading stabilized the cascade for the Mach numbers considered.

(2) A relatively high amount of alternate mistuning is required to have an effect on the stability of the cascade for the Mach numbers considered.

(3) The steady loading due to the airfoil shape and angle of attack increased the blade response compared to that for a flat plate.

(4) An accurate steady solution called "low loss solution " is required for the unsteady solver LINFLX2D to work. This requires a considerable amount of computational time. This may be the biggest drawback of using this code in a design cycle.

(5) The success of getting an unsteady solution from LINFLX2D also depended on the grids used.

(6) For predicting flutter boundary, calculations have to be done for a range of reduced frequencies. It is suggested that LINFLX2D data base be prepared for three or four reduced frequencies, and then use interpolation for flutter calculations. These reduced frequency values can be selected by first running MISER with linear theory.

(7) The unsteady aerodynamic solution times varied from 20 minutes to 75 minutes on an SGI workstation. This is directly related to the number of iterations required for convergence. A solution for flat plate geometry took more time than for the C10 airfoil geometry.

(8) The LINFLX2D code can be used with any aeroelastic code that uses a typical section aeroelastic model as its basis. It can be used with the NASA Glenn Research Center codes ASTROP2, and FREPS with little modification.

REFERENCES

(1) Reddy, et al, "A review of Recent Aeroelastic Analysis Methods for Propulsion at NASA Lewis Research Center", NASA TP 3406, December 1993.

(2) Whitehead, D.S., "Classical Two-Dimensional Methods", Chapter II in AGARD Manual on Aeroelasticity in Axial Flow in Turbomachines, Vol. 1, Unsteady Turbomachinery Aerodynamics, (ed. M. F. Platzer and F. O. Carta), AGARD-AG-298, pp. 3-1:3-30, March 1987.

(3) Smith, S.N., "Discrete Frequency Sound Generation in Axial Flow Turbomachines," British Aeronautical Research Council, London, ARC R&M No. 3709, 1971.

(4) Adamczyk, J.J. and Goldstein, M.E., "Unsteady Flow in a Supersonic Cascade with Subsonic Leading-Edge Locus", ***AIAA Journal***, Vol. 16, No.12, pp. 1248-1254, December 1978.

(5) Surampudi, S.P. and Adamczyk, J.J., "Unsteady Transonic Flow over Cascade Blades", ***AIAA Journal***, Vol. 24, No. 2, Feb. 1986, pp. 293-302.

(6) Lane, F., "Supersonic Flow past an Oscillating Cascade with Supersonic Leading-Edge Locus", ***Journal of the Aeronautical Sciences***, Vol. 24, pp. 65-66, January 1957.

(7) Kaza, K.R.V. and Kielb, R.E., "Flutter and Response of a Mistuned Cascade in Incompressible Flow," ***AIAA Journal***, Vol. 20, No. 8, pp. 1120-1127, 1982.

(8) Kielb, R.E. and Kaza, K.R.V., "Aeroelastic Characteristics of a Cascade of Mistuned Blades in Subsonic and Supersonic Flows", ***ASME Journal of Vibration, Acoustics, Stress and Reliability of Design***, Vol. 105, pp. 425-433, October 1983.

(9) Verdon, J.M., "Linearized Unsteady Aerodynamic Theory," Chapter II in AGARD Manual on Aeroelasticity in Axial Flow in Turbomachines, Vol. 1, Unsteady Turbomachinery Aerodynamics, (ed. M. F. Platzer and F. O. Carta), AGARD-AG-298, pp. 2-1:2-31, March 1987.

(10) Verdon, J.M. and Caspar, J.R., "Development of a Linear Unsteady Aerodynamic Analysis for Finite Deflection Subsonic Cascades", ***AIAA Journal***, Vol. 20, pp. 1259-1267, 1982.

(11) Hoyniak, D., Verdon, J.V., "Steady and Linearized Unsteady Transonic Analyses of Turbomachinery Blade Rows", 7th International Symposium on Unsteady Aerodynamics and Aeroelasticity of Turbomachines, Fukuoka, Japan, Sept. 25-29, 1994, Y. Tanida and M. Namba (editors), pp. 109-124, 1995, Published by Elsevier Science B.V.

(12) Smith, T.E. and Kadambi, J.R., "The Effect of Steady Aerodynamic loading on the Flutter Stability of Turbomachinery Blading", ***Journal of Turbomachinery***, Vol. 115, No. 1, pp. 167-174, 1993.

(13) Hall, K.C. and Clark, W.S., "Linearized Euler Predictions of Unsteady Aerodynamic Loads in Cascades", ***AIAA Journal***, vol. 31, No. 3, pp. 540-550, March 1993.

(14) Holmes, D.G. and Chuang, H.A., "2D Linearized Harmonic Euler Flow Analysis for Flutter and Forced Response", Unsteady Aerodynamic, Aeroacoustics, and Aeroelasticity of Turbomachines and Propellers, pages 213-230, Ed. Atassi, H.M, Springer-Verlag, New York, 1993.

(15) Kahl, G. and Klose, A., "Computation of Time Linearized Transonic Flow in Oscillating Cascades", ASME Paper 93-GT-269, 38th IGT and Aeroengine Congress and Exposition, Cincinnati, Ohio, May 24-27, 1993.

(16) Verdon, J.V., Montgomery, M.D. and Kousen, K.A., "Development of a Linearized Unsteady Euler Analysis for Turbomachinery Blade Rows", NASA CR 4677, June 1995.

(17) Swafford, T.W., et al, "The Evolution of NPHASE: Euler/ Navier-Stokes Computations of Unsteady Two Dimensional Cascade Flow Fields", AIAA Paper 94-1834, 12th Applied Aerodynamics Conference, Colorado Springs, Colorado, June 20-23, 1994.

(18) Lane, F., "System Mode Shapes in the Flutter of Compressor Blade Rows," ***Journal of the Aeronautical Sciences***, Vol. 23, pp. 54-66, January 1956.

(19) Verdon, J.M., "The Unsteady Aerodynamic Response to Arbitrary Modes of Blade Motion", ***Journal of Fluids and Structures***, Vol. 3, pp. 255-274, 1989.

(20) Capece, V., personal communication, University of California, Davis, 1997.

APPENDIX A

Calculated results from the current Version of MISER

Over the years, many versions of MISER code have been in circulation. The present authors also made some modifications to MISER. An important one was updating calls for numerical routines from IMSL 9 to IMSL 10 and LAPACK numerical packages. So, calculations are shown in this appendix to confirm that the authors' MISER code gives the same results as the MISER code used in Ref. 7 in 1982.

Flutter and forced response results are reproduced here by running the current version of the MISER code for the example cases given in Ref. 7. A 56 blade rotor representative of a compressor stage is used. The stagger angle is 54.4 degrees and the gap to chord ratio (s/c) is 0.534. The structural properties are the mass ratio, μ, is 258.50, ratio of bending to torsion frequencies ω_h / ω_α is 0.357, the radius of gyration about the elastic axis in semi-chord units r_α is 0.5774, with no structural damping. The elastic axis is at midchord i.e. ah = 0.0. The distance between the elastic axis and center gravity, x_α is zero. Thus coupling between bending and torsion is very weak, and the flutter mode is dominated by torsional motion. Therefore, only the torsion mode is shown for all the calculations. The flow is considered incompressible.

Figure A.1 shows the root locus plot obtained with and without mistuning for k_b = 0.6425, and for zero structural damping. These results are identical with Fig. 4 in Ref .7.

In figures A2 and A3, aeroelastic response for two engine orders, R = 11 and 39, are presented. These engine orders correspond to interblade phase angles of 70.7 and 250.7 degrees respectively. An alternate mistuning of 1%, and a structural damping of 0.002 is used in the calculations, with k_b = 1.2. These figures are identical with those shown as Fig. 11a and 11b of Ref. 7.

Table 1

Unsteady Aerodynamic Force Coefficients

s/c = 1.0, stagger = 45°, σ = 180°, k_b = 0.5, pitching about midchord (x0=0.5); steady angle of attack is zero for flat plate, 10 degrees for M=0.7 and 13 degrees for M=0.8 for C10 airfoil.

Geometry / Flow condition	Force Coefficient	code	Plunging Real, imaginary	Pitching Real, Imaginary	Vortical gust Real, Imaginary
Flat plate cascade, M= 0.7	cl	a	-3.5675,1.2945	-4.2440,0.7351	1.5768,-2.8183
		b	-3.5133,1.2338	-4.1786,0.6609	1.5684,-2.7637
	cm	a	0.5595,-0.6765	0.7138,-0.8777	-0.1496,0.5944
		b	0.5297,-0.6417	0.6780,-0.8324	-0.1409,0.5648
C10 cascade M = 0.7	cl	a	-3.5675,1.2946	-4.2439,0.7351	1.5768,-2.8183
		b	-2.5502,-0.0132	-2.2566,-0.1537	4.7945,-4.6932
		c	-2.6370,0.0553	-2.3040,-0.0487	**
		d	-2.6576,0.0310	-2.4415,-0.0362	**
	cm	a	0.5595,-0.6765	0.7138,-0.8777	-0.1496,0.5944
		b	0.6497,-0.3330	0.6001,-0.4540	-0.5963,0.4450
		c	0.6124,-0.3340	0.5513,-0.4406	**
		d	0.6346,-0.3474	0.5917,-0.5108	**
C10 cascade M = 0.8	cl	a	-0.4792,2.6405	-0.4467,3.1039	-0.5932,-2.1091
		b	*	*	*
		c	-2.5945,1.0469	-1.8953,0.8885	**
		d	-2.7240,1.1272	-2.0532,0.9119	**
	cm	a	-0.4633,0.03245	-0.7879,-0.1658	0.02522,-0.2289
		b	*	*	*
		c	0.3352,-0.6922	0.2215,-0.6712	**
		d	0.3615,-0.6567	0.2657,-0.6940	**

a = linear theory, Ref. 3;
b = LINFLX2D (155x41 grid with 55 points on the airfoil, inlet=-1.0, exit=+2.0)
c = LINFLX2D (141x41 grid with 81 points on the airfoil, inlet=-5.0, exit=+10.00)
d = nonlinear unsteady Euler code, Ref. 17
* could not get solution with 155x41 grid; ** did not run for gust predictions

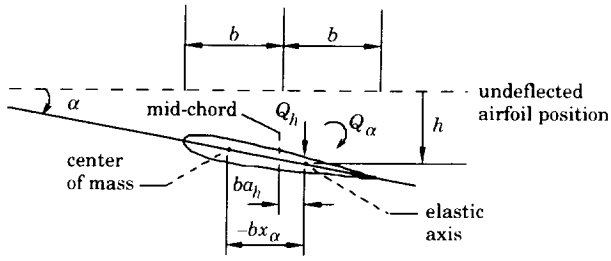

Figure 1: Typical section blade model with two degrees-of-freedom.

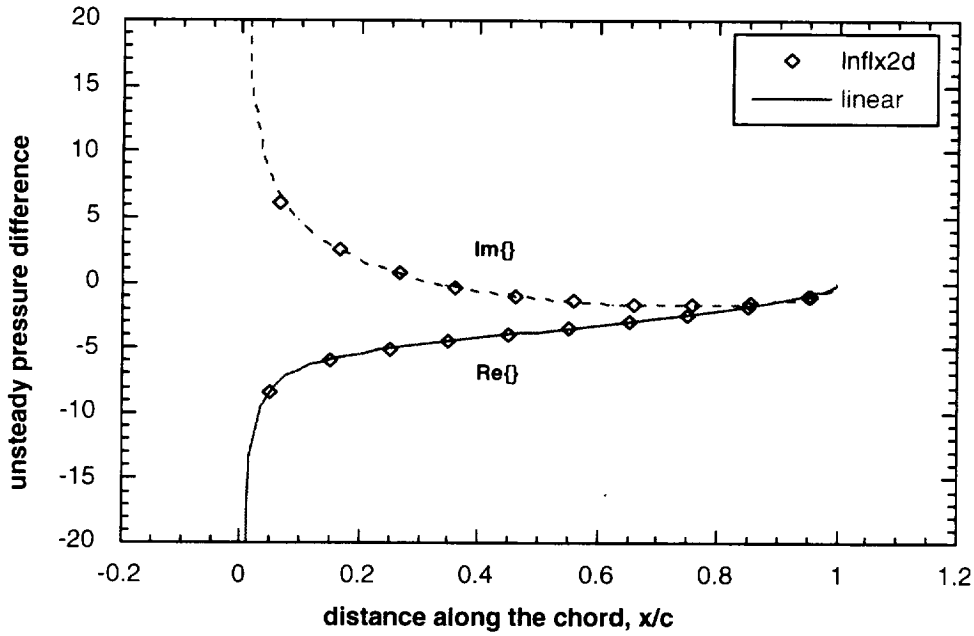

Figure 2a: Unsteady pressure difference distribution for a flat plate geometry cascade; pitching about mid-chord; gap-to-chord ratio, s/c = 1.0, stagger angle, $\theta = 45°$, free stream Mach number, M = 0.7, steady angle of attack, $i = 0°$, reduced frequency based on semi-chord, $k_b = 0.5$, interblade phase angle, $\sigma = 180°$, amplitude of oscillation, $\alpha_O = 2°$.

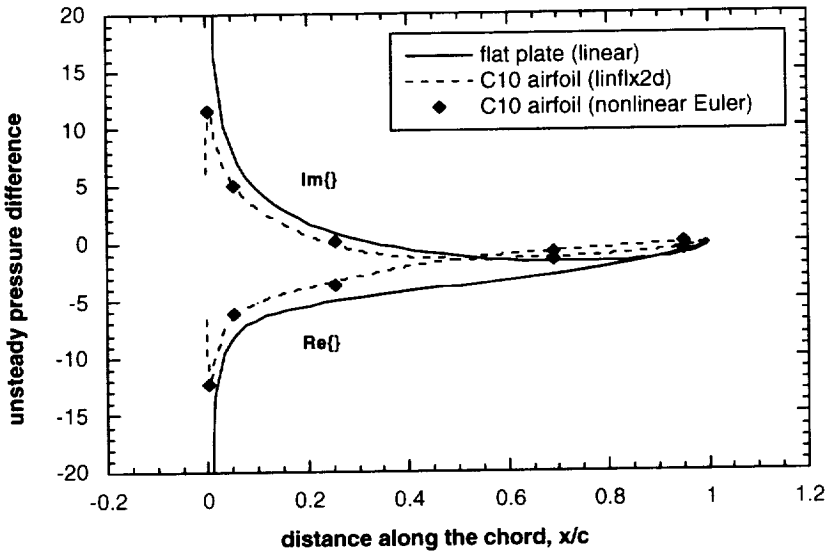

Figure 2b: Unsteady pressure difference distribution for a subsonic cascade, pitching about midchord; , $s/c = 1.0$, $\theta = 45°$, $M = 0.7$, $k_b = 0.5$, $\sigma = 180°$, $\alpha_o = 2°$, $i = 0°$ for flat plate and $i = 10°$ for C10 airfoil.

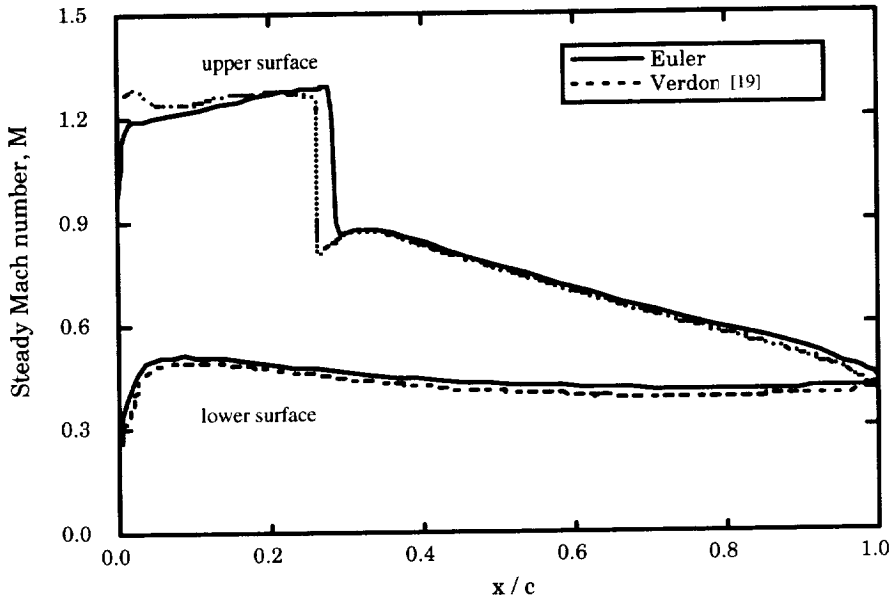

Figure 3a: Steady Mach number distribution for a transonic cascade; standard configuration No. 10, $s/c = 1.0$, $\theta = 45°$, $M = 0.8$, $i = 13°$.

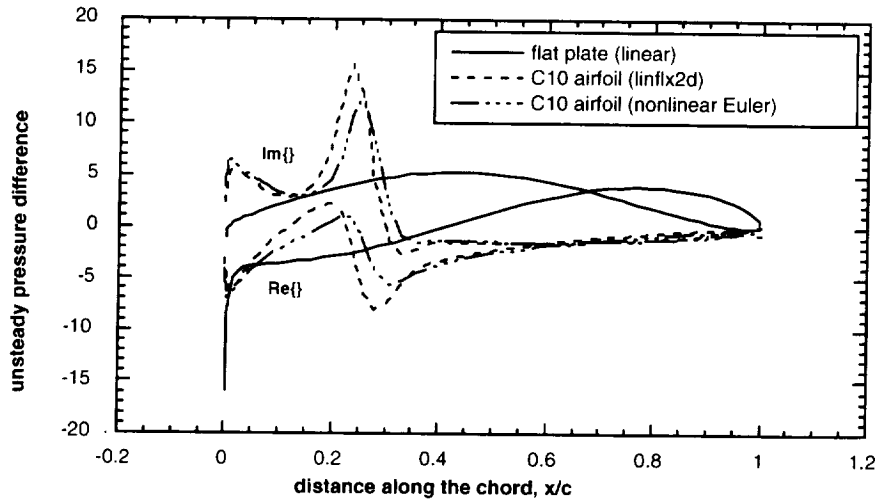

Figure 3b: Unsteady pressure difference distribution for a transonic cascade; standard configuration No. 10, pitching about mid-chord; parameters as in Fig. 3a, $k_b = 0.5$, $\sigma = 180°$, $\alpha_0 = 2°$.

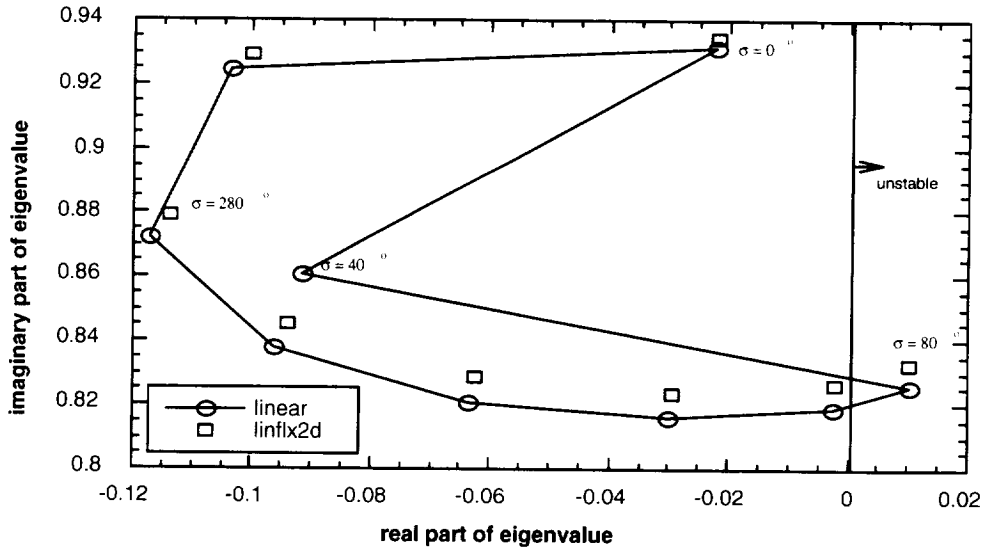

Figure 4: Root locus plot for 9 bladed cascade, torsional motion, flat plate geometry, $k_b = 0.18$, $a_h = 0.0$, $\mu = 258.5$, $r_\alpha = 0.5774$, structural damping=0.0, $\omega_h / \omega_\alpha = 0.357$, M = 0.7, $i = 0°$

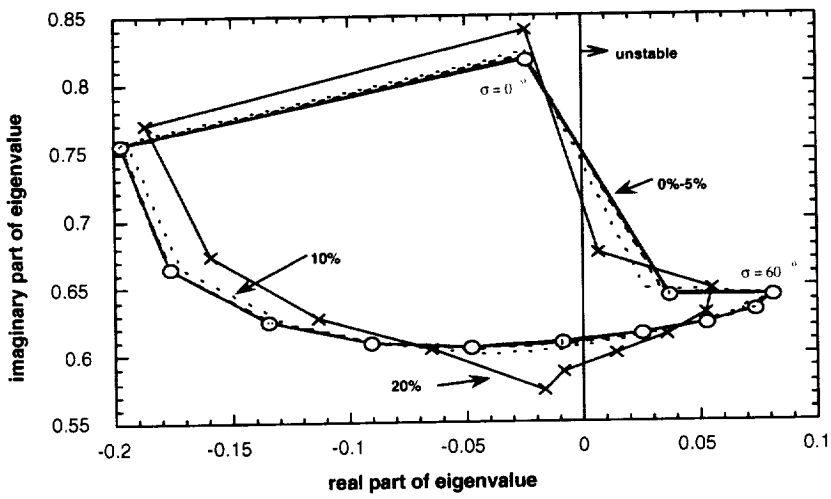

Figure 5: Effect of alternate mistuning on eigenvalues in subsonic flow; flat plate geometry, $M = 0.7$, $i = 0°$, $k_b = 0.1$, N=12, pitching about mid-chord; .1%,2%,5%,10%, 20%; structural parameters same as in Fig. 4.

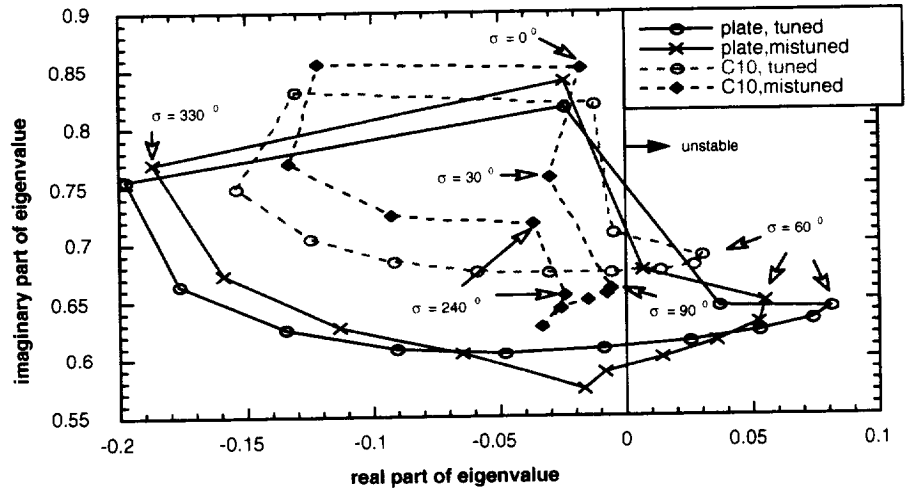

Figure 6: Effect of alternate mistuning on eigenvalues in subsonic flow; standard configuration No. 10, $M = 0.7$, $i = 10°$, $k_b = 0.1$, N = 12, pitching about mid-chord; structural parameters same as in Fig. 4.

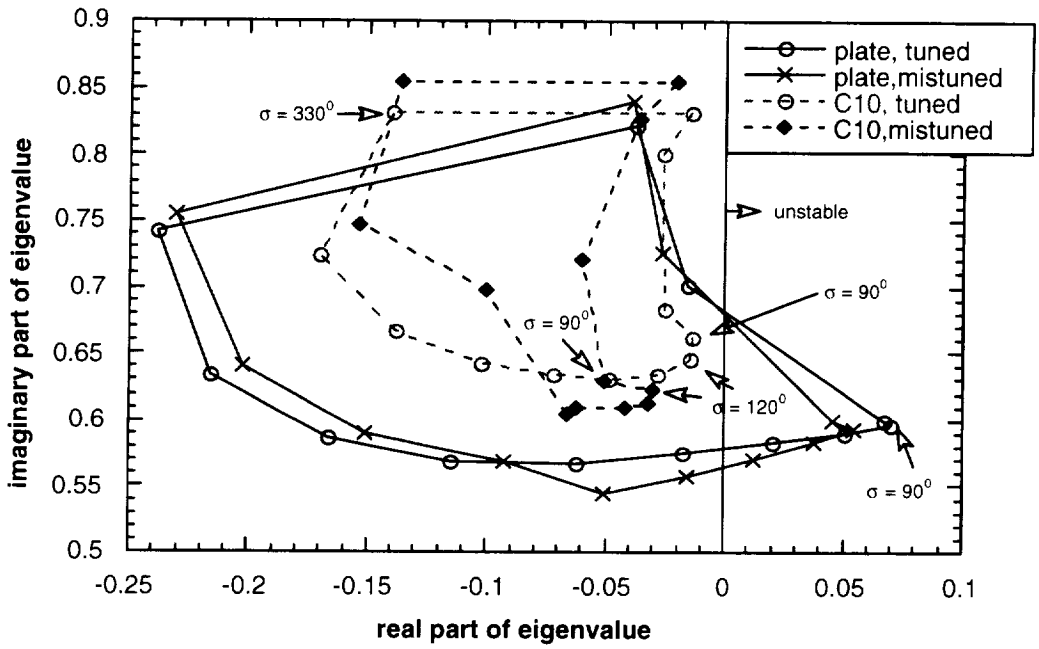

Figure 7: Effect of alternate mistuning on eigenvalues in transonic flow; standard configuration No. 10, $M = 0.8$, $i = 13°$, $k_b = 0.1$, N = 12, pitching about mid-chord; structural parameters same as in Fig. 4.

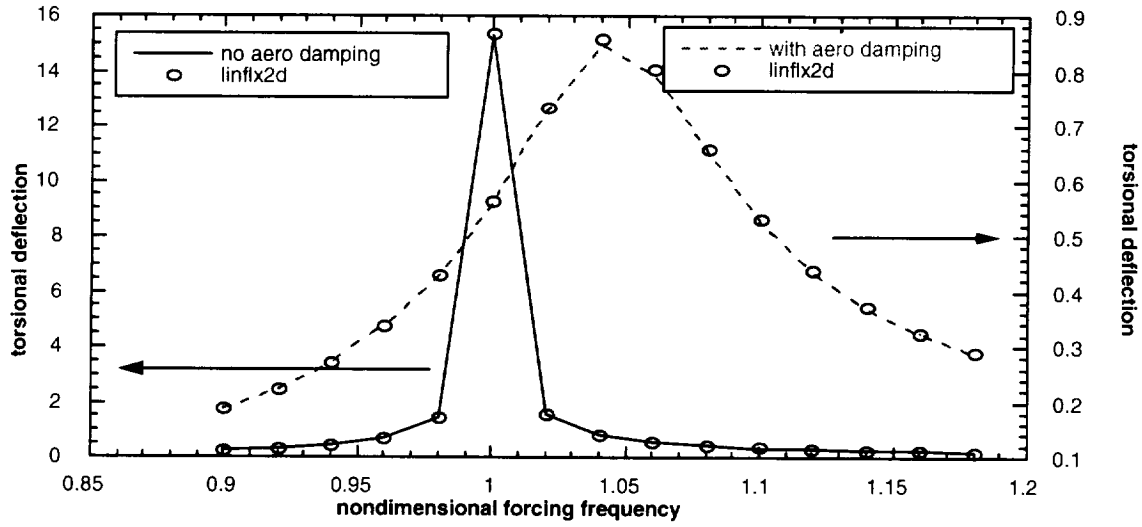

Figure 8: Comparison of torsional response for a tuned cascade; flat plate geometry, $M = 0.7$, $i = 0°$, $k_b = 0.5$, N = 12, pitching about leading edge; structural damping ratio = 0.002; structural parameters same as in Fig. 4. Lines are calculations from linear theory.

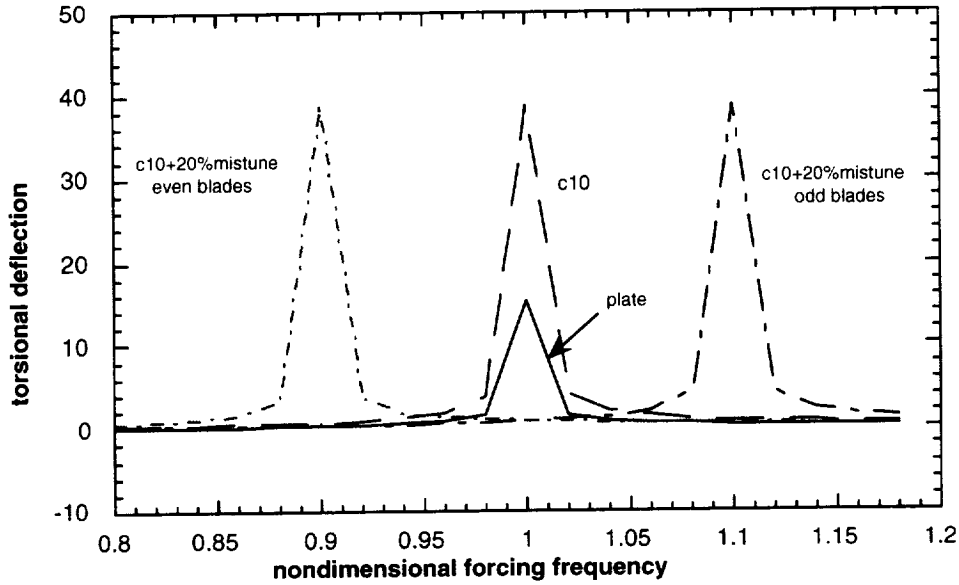

Figure 9: Effect of steady loading on torsional response, $M = 0.7$, $i = 0°$, $k_b = 0.5$, N = 12, pitching about leading edge; structural damping ratio = 0.002; structural parameters same as in Fig. 4.

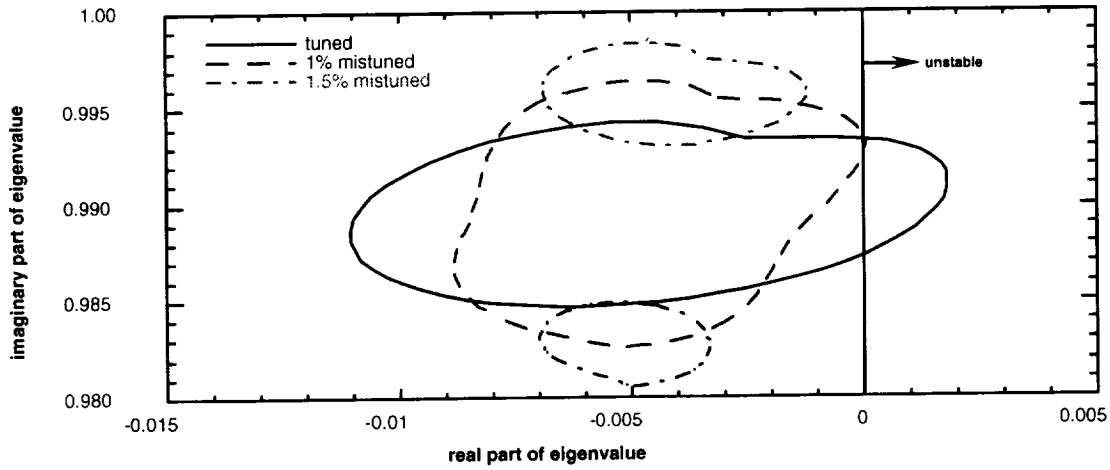

Figure A 1: Effect of alternate mistuning on eigenvalues in incompressible flow; flat plate, incompressible flow, $i = 0°$, $k_b = 0.642$, N = 56, pitching about mid-chord; structural parameters same as in Fig. 4 (identical with Fig.5 of Ref. 7).

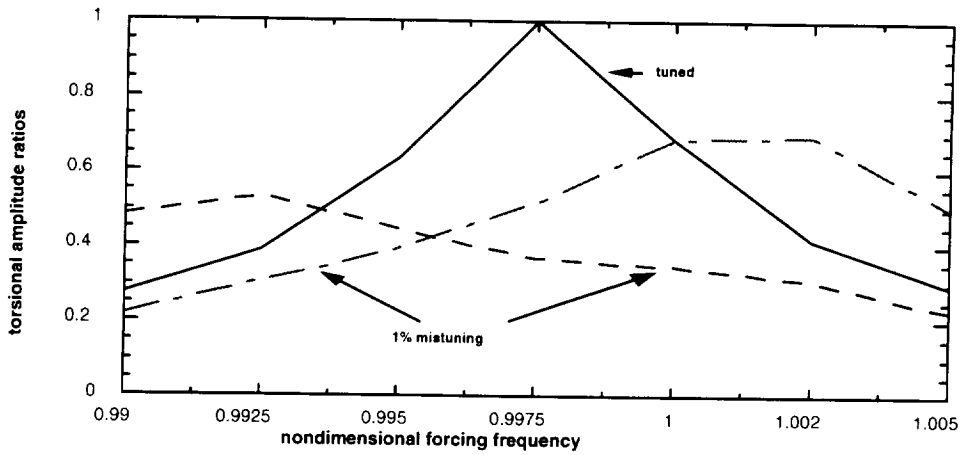

Figure A.2: Effect of blade alternate mistuning on coupled bending-torsion response in incompressible flow; flat plate, incompressible flow, $i = 0°$, $k_b = 1.2$, N = 56, R = 11, pitching about mid-chord; structural damping ratio = 0.002; structural parameters same as in Fig. 4 (identical with Fig. 11a of Ref. 7).

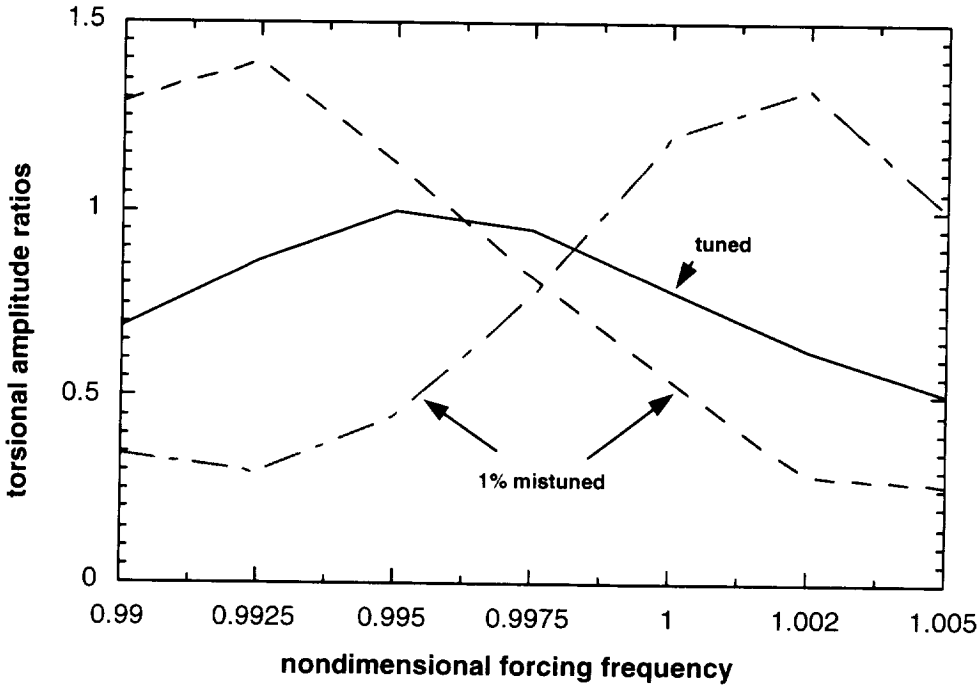

Figure A.3: Effect of blade alternate mistuning on coupled bending-torsion response in incompressible flow; flat plate, incompressible flow, $i = 0°$, $k_b = 1.2$, N = 56, R = 39, pitching about mid-chord; structural damping ratio = 0.002; structural parameters same as in Fig. 4 (identical with Fig. 11b of Ref. 7)

REPORT DOCUMENTATION PAGE

Form Approved
OMB No. 0704-0188

1. AGENCY USE ONLY (Leave blank)	2. REPORT DATE	3. REPORT TYPE AND DATES COVERED
	November 1999	Technical Memorandum

4. TITLE AND SUBTITLE

Flutter and Forced Response Analyses of Cascades Using a Two-Dimensional Linearized Euler Solver

5. FUNDING NUMBERS

WU-523-26-13-00

6. AUTHOR(S)

T.S.R. Reddy, R. Srivastava, and O. Mehmed

7. PERFORMING ORGANIZATION NAME(S) AND ADDRESS(ES)

National Aeronautics and Space Administration
John H. Glenn Research Center at Lewis Field
Cleveland, Ohio 44135-3191

8. PERFORMING ORGANIZATION REPORT NUMBER

E-11960

9. SPONSORING/MONITORING AGENCY NAME(S) AND ADDRESS(ES)

National Aeronautics and Space Administration
Washington, DC 20546-0001

10. SPONSORING/MONITORING AGENCY REPORT NUMBER

NASA TM—1999-209633

11. SUPPLEMENTARY NOTES

T.S.R. Reddy and R. Srivastava, The University of Toledo, Toledo, Ohio 43606; O. Mehmed, NASA Glenn Research Center. Responsible person, O. Mehmed, organization code 5930, (216) 433-6036.

12a. DISTRIBUTION/AVAILABILITY STATEMENT

Unclassified - Unlimited
Subject Category: 39 Distribution: Nonstandard

This publication is available from the NASA Center for AeroSpace Information, (301) 621-0390.

12b. DISTRIBUTION CODE

13. ABSTRACT ***(Maximum 200 words)***

Flutter and forced response analyses for a cascade of blades in subsonic and transonic flow is presented. The structural model for each blade is a typical section with bending and torsion degrees of freedom. The unsteady aerodynamic forces due to bending and torsion motions, and due to a vortical gust disturbance are obtained by solving unsteady linearized Euler equations. The unsteady linearized equations are obtained by linearizing the unsteady nonlinear equations about the steady flow. The predicted unsteady aerodynamic forces include the effect of steady aerodynamic loading due to airfoil shape, thickness and angle of attack. The aeroelastic equations are solved in the frequency domain by coupling the unsteady aerodynamic forces to the aesroelastic solver MISER. The present unsteady aerodynamic solver showed good correlation with published results for both flutter and forced response predictions. Further improvements are required to use the unsteady aerodynamic solver in a design cycle.

14. SUBJECT TERMS	15. NUMBER OF PAGES
Flutter; Forced response; Cascades; Euler; Linearized; Mistuned	31
	16. PRICE CODE: A03

17. SECURITY CLASSIFICATION OF REPORT	18. SECURITY CLASSIFICATION OF THIS PAGE	19. SECURITY CLASSIFICATION OF ABSTRACT	20. LIMITATION OF ABSTRACT
Unclassified	Unclassified	Unclassified	